

A Stochastic Gravitational Wave Background Coming from a Double Peak Domain Wall Model

Catalina-Ana Miritescu,^{a,*} Adrian Macquet,^a Mario Martinez Perez,^{a,b} Ricardo Zambujal Ferreira^a and Oriol Pujolas^a

^a*Institut de Física d'Altes Energies (IFAE),
Campus UAB, Facultat Ciències Nord, Bellaterra, Barcelona, Spain*

^b*Catalan Institution for Research and Advanced Studies (ICREA),
Passeig de Lluís Companys, 23, Barcelona, Spain*

E-mail: cmiritescu@ifae.es

We performed an agnostic search in the data from the first three observing runs of LIGO - Advanced LIGO and Virgo - Advanced Virgo for a novel model of stochastic gravitational waves background (SGWB). The SGWB power spectrum is produced, in this case, by a superposition of the stochastic compact binary coalescence signals (CBCs) and a double-peaked gravitational waves domain wall model. The two peaks were characterized using broken power-law models. We placed a 95% confidence level upper limits on the gravitational wave energy density at 25Hz from CBCs and, simultaneously, on the amplitude of the two peaks. Detection prospects using these upper limit values are discussed for third generation detectors, such as the Einstein Telescope.

*The European Physical Society Conference on High Energy Physics (EPS-HEP2023)
21-25 August 2023
Hamburg, Germany*

*Speaker

1. Introduction

A stochastic gravitational wave background (SGWB) refers to a superposition of gravitational waves (GWs) with a broad range of frequencies and amplitudes, resulting in a seemingly random or "stochastic" pattern. The sources of stochastic gravitational wave backgrounds can either be astrophysical – a superposition of large numbers of independent, unresolved compact binary coalescence signals – or cosmological such as inflation, phase transitions, cosmic strings, and topological defects in the early universe.

While recent observations of such a background have been obtained through the Pulsar Timing Array (PTA) projects (North American Nanohertz Observatory for Gravitational Waves (NANOGrav) [1], European Pulsar Timing Array (EPTA) [2] and Parkes Pulsar Timing Array (PPTA) [3]) in the nanohertz frequency range, no detection has been achieved so far with ground based interferometers, which have their peak sensitivity in the $10\text{Hz} - 1000\text{Hz}$ frequency range. Depending on the source, different models of gravitational waves power spectra can be predicted and constraints can be placed on the model's parameters based on the available observations.

2. Motivation

A stochastic gravitational wave background power spectrum can be modelled from cosmic domain walls (DW). They are two-dimensional topological defects predicted by several theories beyond the standard model, and are expected to arise from the spontaneous breaking of a discrete symmetry in the early universe. Soon after formation, their energy density would dominate the total energy density of the universe, which contradicts current observations. Thus, an annihilation mechanism for domain walls is needed.

In Refs. [4–6] it is argued that the collapse of domain walls could give rise to long-lived, non-perturbative oscillating energy concentrations – oscillons. Both the DW network annihilation and the resulting oscillons radiate gravitational waves. While the DW GW spectrum has been modelled and searched for before in the O1+O2+O3 LVK data [7], we now add a second feature due to the presence of oscillons.

3. Parametrization

The total SGWB power spectrum is modelled here as the sum of the compact binary coalescence signals (CBCs), the domain wall contribution (DW) and the oscillon feature, which we will call the second peak (SP).

$$\Omega(f) = \Omega_{CBC} + \Omega_{DW} + \Omega_{SP}$$

We will use the parametrization from [8] to describe both the peak corresponding to DW annihilation and the second peak corresponding to oscillon radiation, while the CBC will take the usual power law form:

$$\Omega(f) = \Omega_{ref} \left(\frac{f}{f_{ref}} \right)^\alpha + \Omega_{*1} S \left(\frac{f}{f_{*1}} \right) + \Omega_{*2} S \left(\frac{f}{f_{*2}} \right)$$

$$S\left(\frac{f}{f_{*1,2}}\right) = \frac{(\gamma_{1,2} + \beta_{1,2})^{\delta_{1,2}}}{\left(\beta_{1,2} \left(\frac{f}{f_{*1,2}}\right)^{-\frac{\gamma_{1,2}}{\delta_{1,2}}} + \gamma_{1,2} \left(\frac{f}{f_{*1,2}}\right)^{\frac{\beta_{1,2}}{\delta_{1,2}}}\right)^{\delta_{1,2}}}$$

Here, γ describes the behaviour of the function at low frequencies, while β describes the behaviour at high frequencies, and δ is the width around the maximum.

Some parameters can be fixed due to physical constraints ($\gamma_1 = 3$ due to causality [9]), while others have been determined from numerical simulations for a single peak domain wall model ($\beta_1 = 1, \delta_1 = 1$ [10]). While the addition of the second peak changes the values of β_1 and $\delta_1 = 1$, we keep the same spectral slope behaviour for high frequencies ($\beta_2 = 1$). The CBC background uses the usual values for $\alpha = \frac{2}{3}$ and $f_{ref} = 25Hz$. Thus we are left with 9 free parameters.

4. Search

4.1 Wide Search

We need to select priors for all the free parameters and then perform a Bayesian analysis using the O1+O2+O3 LVK data and the Bilby library [11].

The amplitude of the CBC stochastic background emission and the two peak amplitudes were sampled in a *log – uniform* fashion, while the frequencies and the exponents were sampled in a *linear – uniform* way (Table 1). The amplitudes range was chosen to contain the most recent upper limit estimations. The frequency range was chosen to correspond to the peak sensitivity of the LIGO-Virgo detectors.

Param.	Prior type	Prior range
Ω_{ref}	LogUniform	$(10^{-10}, 10^{-6})$
Ω_{1*}	LogUniform	$(10^{-10}, 10^{-6})$
f_{1*}	Uniform	$(20Hz, 200Hz)$
Ω_{2*}	LogUniform	$(10^{-10}, 10^{-6})$
f_{2*}	Uniform	$(20Hz, 200Hz)$
β_1	Uniform	$(1, 9)$
γ_2	Uniform	$(1, 9)$
δ_1	Uniform	$(0.1, 1)$
δ_2	Uniform	$(0.1, 1)$

Table 1: Priors selected for the wide search.

It is worth noting that a few additional constraints were implemented in this search. The amplitude of the second peak Ω_{2*} was considered to be smaller than the amplitude of the first peak Ω_{1*} (this condition produces the diagonal feature in the Ω_{1*} vs. Ω_{2*} plots in Figures 1 and 2). The central frequency of the second peak f_{2*} was chosen to be at least $20Hz$ greater than the central frequency of the first peak f_{1*} , in order for the function to exhibit two distinguishable peak features and not to be confused with a simple broken power law corresponding solely to domain wall annihilation (this condition gives rise to the diagonal feature present in the f_{1*} vs. f_{2*} plots in Figures 1 and 2). For the same reason, we focused our search on low values for δ_1 and δ_2 - the smaller the width around the maximum, the sharper the peak and the easier it would be to detect it.

The posterior distributions of the parameters for the Bayesian search in O1+O2+O3 data using the priors described in the table above are presented in Figure 1. For the amplitudes, we obtain the following upper limits, with a 95% confidence level: $\Omega_{ref} = 5.5 \times 10^{-9}$, $\Omega_{1*} = 3.5 \times 10^{-8}$, and

$\Omega_{2*} = 6.6 \times 10^{-9}$. These values are compatible with the results obtained in the LVK O3 stochastic gravitational waves background search paper [12], where the numerical value for Ω_{ref} was found to be $\Omega_{ref} = 3.4 \times 10^{-9}$. For the exponents, we obtain flat posteriors, indicating no preference for any particular value. Thus, in the following search (Figure 2) we fix the values of these parameters.

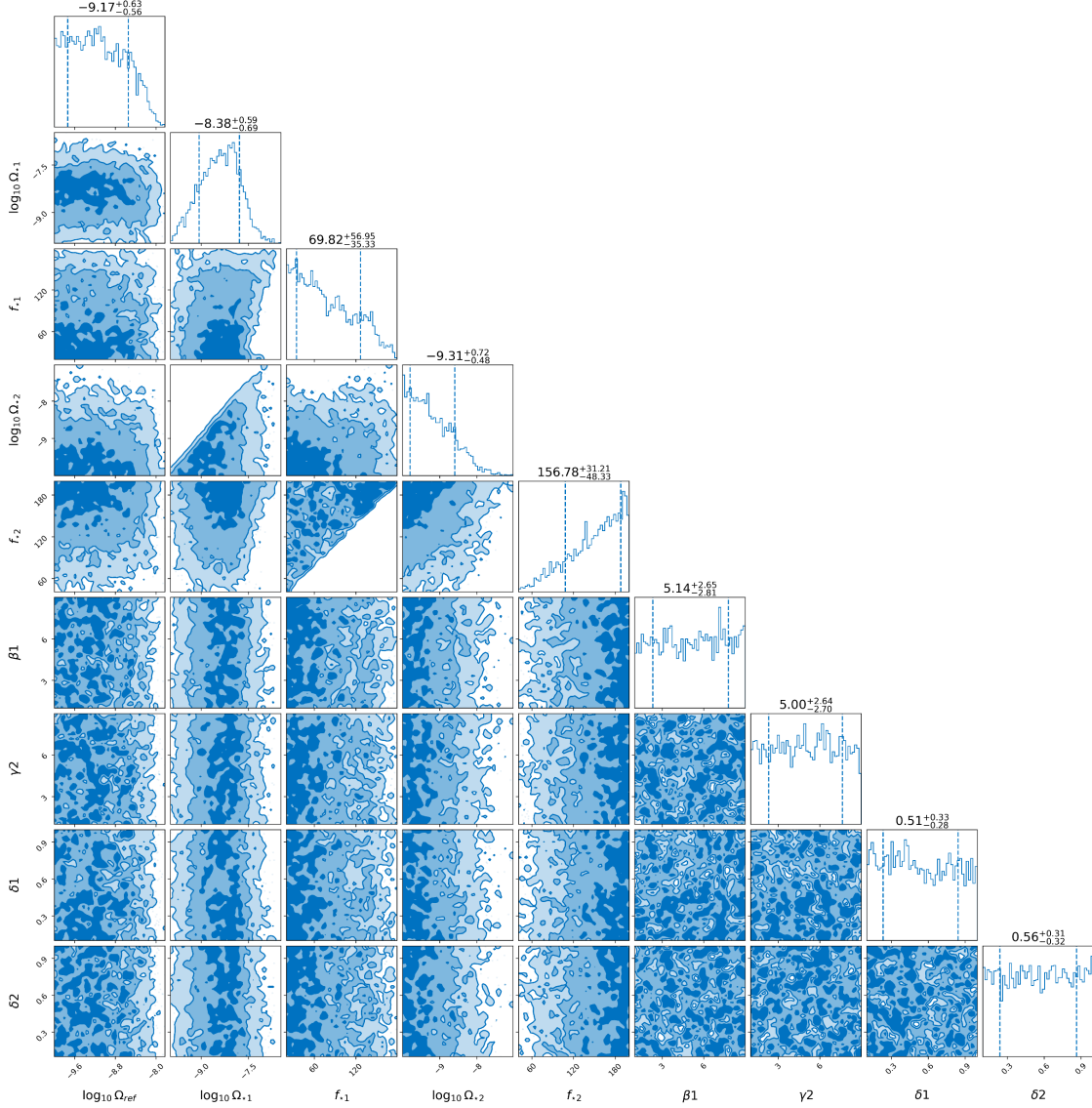


Figure 1: Corner plot results for the Bayesian search using the parameters described above.

The Bayes factor calculated between a model containing only noise and the model composed of the CBC + DW + SP gravitational waves stochastic background has the value:

$$\log B_{Noise}^{CBC+DW+SP} = -1.98$$

We can thus conclude for this search that there is no evidence to support this model over a purely Gaussian noise one.

4.2 Benchmark Search

As the exponents' posteriors were flat in the previous search, we selected constant values for them to perform a benchmark Bayesian analysis: $\beta_1 = 1$, $\gamma_2 = 3$, (motivated by the causality and numerical simulations previously discussed) $\delta_1 = 0.1$, $\delta_2 = 0.1$ (motivated by the desire to have discernible peaks).

Param.	Prior type	Prior range
Ω_{ref}	LogUniform	$(10^{-11}, 10^{-6})$
Ω_{1*}	LogUniform	$(10^{-11}, 10^{-6})$
f_{1*}	Uniform	$(20Hz, 160Hz)$
Ω_{2*}	LogUniform	$(10^{-11}, 10^{-6})$
f_{2*}	Uniform	$(20Hz, 160Hz)$

Table 2: Priors selected for the benchmark search.

O1+O2+O3 data using the priors described in the table above are presented in Figure 2. For the amplitudes, we obtain the following upper limits, with a 95% confidence level: $\Omega_{ref} = 4.85 \times 10^{-9}$, $\Omega_{1*} = 2 \times 10^{-8}$, and $\Omega_{2*} = 2.3 \times 10^{-9}$.

The priors for the other parameters are presented in Table 2. To increase chances of a possible detection, we further decreased the prior range of the two frequencies to the least noisy interval in LIGO-Virgo: $(20Hz, 160Hz)$. We maintain the conditions previously applied to the frequencies and to the amplitudes of the two peaks.

The posterior distributions of the parameters for the Bayesian search in

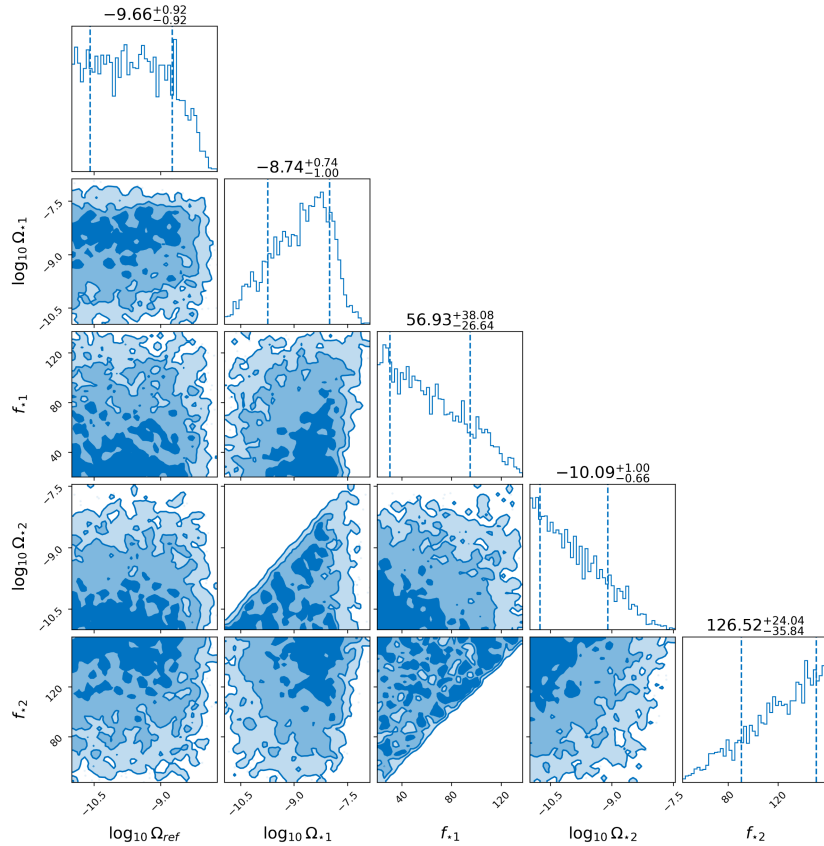


Figure 2: Corner plot results for the Bayesian benchmark analysis.

Calculating the Bayes factor for this configuration vs. noise, one obtains:

$$\log B_{\text{Noise}}^{\text{CBC+DW+SP}} = -1.49$$

Once again, there is no evidence for a signal described by the above parametrization, even when considering the most favorable case.

5. Discussion

With the construction of 3rd generation GW detectors such as the Einstein Telescope (ET) in Europe and Cosmic Explorer (CE) in the US, an increased sensitivity is expected and the detection of a SGWB will hopefully be achieved (see Figure 3).

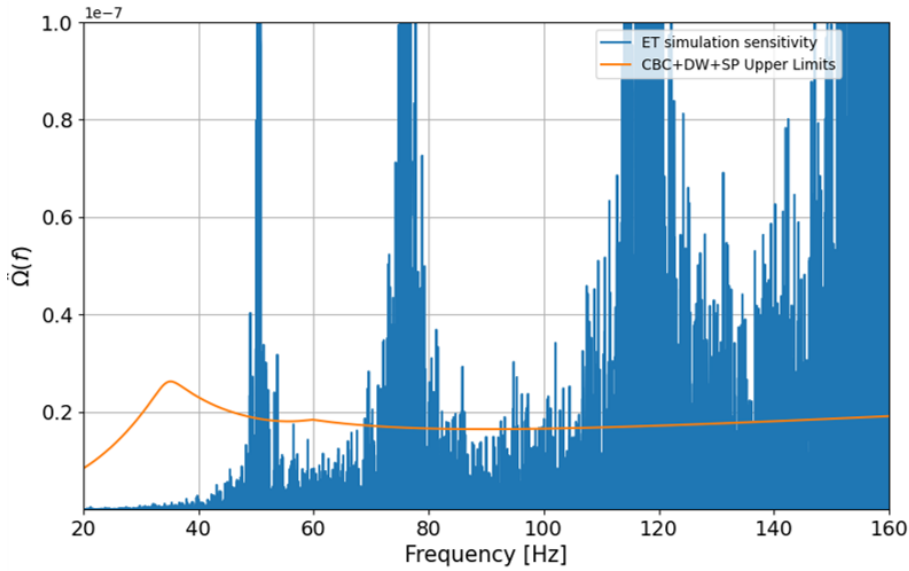


Figure 3: Example of a SGWB power spectrum corresponding to the parametrization discussed in this paper (orange) plotted on top of the simulated cross-correlation noise expected for ET (blue).

In the plotted example, the upper limits from Figure 2 have been used. f_{1*} was chosen to be 35Hz , and f_{2*} was chosen to be 60Hz . If the physical values of the SGWB power spectrum are close to the upper limits, we expect a detection (the signal being well above the noise). If no detection will be achieved, new upper limits will be calculated and stronger constraints will be placed on the parameters of the model.

As future work, a phenomenological parametrization of the two peaks will be implemented, with the first peak of the SGWB power spectrum depending on parameters such as the annihilation temperature of the domain walls T_* , the number of relativistic degrees of freedom g_* , the domain wall surface energy density σ [8], while the exact phenomenological parametrization of the second peak is still under development.

While the analysis performed in this work was motivated by the expected behaviour of domain walls networks and oscillons, other combinations of cosmological phenomena could give rise to a

double-peaked SGWB power spectrum. The agnostic parametrization used here could be relevant in those situations.

References

- [1] Gabriella Agazie et al. The nanograv 15 yr data set: Evidence for a gravitational-wave background. *The Astrophysical Journal Letters*, **951**, Jun 2023.
- [2] EPTA Collaboration and InPTA Collaboration:. The second data release from the european pulsar timing array - iii. search for gravitational wave signals. *A&A*, **678**:A50, 2023.
- [3] Daniel J. Reardon et al. Search for an isotropic gravitational-wave background with the parkes pulsar timing array. *The Astrophysical Journal Letters*, **951**(1):L6, jun 2023.
- [4] Mark Hindmarsh and Petja Salmi. Oscillons and domain walls. *Phys. Rev. D*, **77**:105025, May 2008.
- [5] Alejandro Vaquero, Javier Redondo, and Julia Stadler. Early seeds of axion miniclusters. *Journal of Cosmology and Astroparticle Physics*, **2019**(04):012, Apr 2019.
- [6] Naoya Kitajima, Fumiaki Kozai, Fuminobu Takahashi, and Wen Yin. Power spectrum of domain-wall network, and its implications for isotropic and anisotropic cosmic birefringence. *Journal of Cosmology and Astroparticle Physics*, **2022**(10):043, Oct 2022.
- [7] Yang Jiang and Qing-Guo Huang. Implications for cosmic domain walls from the first three observing runs of ligo-virgo. *Phys. Rev. D*, **106**:103036, Nov 2022.
- [8] Ricardo Z. Ferreira, Alessio Notari, Oriol Pujolàs, and Fabrizio Rompineve. Gravitational waves from domain walls in pulsar timing array datasets. *Journal of Cosmology and Astroparticle Physics*, **2023**(02):001, Feb 2023.
- [9] Chiara Caprini et al. Detecting gravitational waves from cosmological phase transitions with LISA: an update. *Journal of Cosmology and Astroparticle Physics*, **2020**(03):024–024, Mar 2020.
- [10] Takashi Hiramatsu, Masahiro Kawasaki, and Ken'ichi Saikawa. On the estimation of gravitational wave spectrum from cosmic domain walls. *Journal of Cosmology and Astroparticle Physics*, **2014**(02):031–031, Feb 2014.
- [11] Gregory Ashton et al. Bilby: A user-friendly bayesian inference library for gravitational-wave astronomy. *The Astrophysical Journal Supplement Series*, **241**(2):27, Apr 2019.
- [12] R. Abbott et al. Upper limits on the isotropic gravitational-wave background from advanced ligo and advanced virgo's third observing run. *Phys. Rev. D*, **104**:022004, Jul 2021.